Determination of the Relative Permittivity, ϵ', of Methylbenzene at Temperatures between (290 and 406) K and Pressures below 20 MPa with a Radio Frequency Re-Entrant Cavity and Evaluation of a MEMS Capacitor for the Measurement of ϵ'

Mohamed E. Kandil and Kenneth N. Marsh

Department of Chemical and Process Engineering, University of Canterbury, Christchurch, New Zealand

Anthony R. H. Goodwin*

Schlumberger Technology Corporation, 125 Industrial Boulevard, Sugar Land, Texas 77478

The relative electric permittivity of liquid methylbenzene has been determined with an uncertainty of 0.01 % from measurements of the resonance frequency of the lowest order inductive-capacitance mode of a re-entrant cavity (*J. Chem. Thermodyn.* **2005**, *37*, 684–691) at temperatures between (290 and 406) K and pressures below 20 MPa and at $T = 297$ K with a MicroElectricalMechanical System (MEMS) interdigitated comb capacitor. For the re-entrant cavity, the working equations were a combination of the expressions reported by Hamelin et al. (*Rev. Sci. Instrum.* **1998**, *69*, 255−260) and a function to account for dilation of the resonator vessel walls with pressure that was determined by calibration with methane (*J. Chem. Eng. Data* **2007**, *52*, 1660–1671). The results were represented by an empirical equation reported by Owen and Brinkley (*Liq. Phys. Rev.* **1943**, *64*, 32–36) analogous to the Tait equation (*Br. J. Appl. Phys.* **1967**, *18*, 965–977) with a standard ($k = 1$) uncertainty of 0.33 %. The values reported by Mospik (*J. Chem. Phys.* **1969**, *50*, 2559–2569) differed from the interpolating equation by $< \pm$ 0.2 % at temperatures that overlap ours; extrapolating the smoothing expression to $T = 223$ K, a temperature of 40 K below the lowest used for the measurements, provided values within $\pm$ 0.6 % of the data reported by Mospik. A parallel plate capacitor is described that was formed from interdigitated combs that were fabricated by the techniques of MEMS. This device has capacitances arising from fringing fields that contributed about 50 % to the total capacitance of about 3 pF. The fringing field was accommodated with a calibration with octane using the data of Scaife and Lyons (*Proc. R. Soc. London A* **1980**, *370*, 193–211, SUP 10031). The values of the relative permittivity of methylbenzene obtained with the MEMS at $T = 297$ K and $p < 40$ MPa deviated systematically from the smoothing equation based on the re-entrant cavity data by between −0.9 % at $p = 7$ MPa and 0.5 % at $p = 42$ MPa within about 5 times the estimated expanded ($k = 2$) uncertainty of the measurements obtained with the MEMS.

Introduction

The optimal recovery of naturally occurring hydrocarbon mixtures depends on knowledge of the physical properties of the porous media and the hydrocarbon contained within. Conventional petroleum reservoirs, which have been the traditional source, contain fluids with densities of about 800 kg·m^{-3} and viscosities on the order of 1 mPa·s at reservoir and production conditions with temperatures less than 473 K at pressures below 200 MPa. For these resources, the required thermophysical properties include phase boundaries, density, and viscosity.

Heavy oil and bitumen are a subset of unconventional hydrocarbons, which comprises more than 50 % of the estimated remaining world's hydrocarbon resource and are consequently of significance to the petroleum industry.[1] Many of the physiochemical properties of these two unconventional hydrocarbon sources differ from conventional oil. The most commonly used distinguishing thermophysical properties are the density

and viscosity. Heavy oil has a hydrocarbon of density between (933 and 999) kg·m^{-3}, about 25 % more dense than conventional oil, and natural bitumen has a density exceeding 1000 kg·m^{-3}. The United Nations Information Centre for Heavy Crude and Tar Sands defines bitumen as petroleum with a viscosity $> 10^4$ mPa·s at reservoir conditions, while heavy oil has a viscosity $< 10^4$ mPa·s. For heavy oil, the reservoir temperatures are less than 323 K and the pressures are below 40 MPa.

Before continuing with the description of measurements, we digress to discuss heavy oil and bitumen. Heavy oil and bitumen require, in addition to the thermophysical properties of conventional oil listed above, the complex permittivity as a function of applied voltage up to material break-down; refs 2 and 3 report that asphalt, a constituent of bitumen and heavy oil, has a relative electric permittivity greater than 2.7, which is 50 % greater than the value for paraffin of about 2 reported by Sen et al.[4] The temperature, pressure, and frequency dependence of the electrical properties are particularly important for the production of heavy oil and bitumen with electromagnetic methods.[5–9] The electrical properties of conventional resources are also of interest

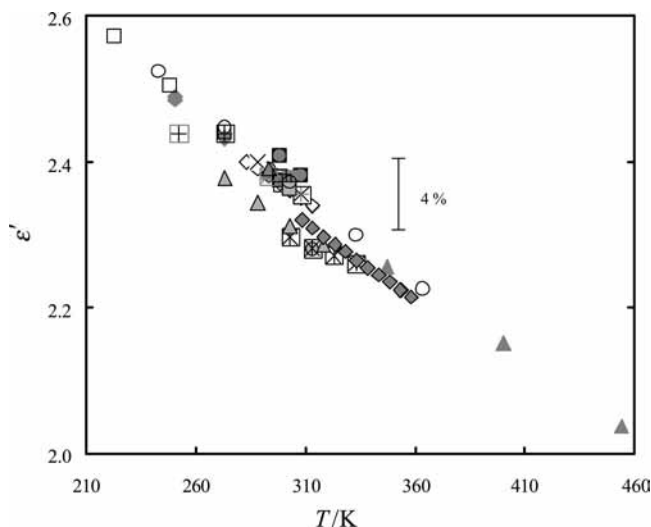* Corresponding author. E-mail: agoodwin@slb.com. Fax: +1 281 285 8071.

Figure 1. Relative electric permittivity $\mathcal{R}(\epsilon_r) \equiv \epsilon'$ of methylbenzene as a function of temperature T at a pressure of 0.1 MPa. At $T \geq 383.75$ K, the normal boiling temperature, measurements were performed at $p > p^{l+g}$ where p^{l+g} is the vapor pressure. Gray-filled triangle with black outline, ref 13; gray-filled and outlined triangle, ref 14; gray cross, ref 15; gray diamond, ref 16; $\triangle$, ref 17; $\bigcirc$, ref 18; $+$, ref 19; gray-filled square, ref 20; light gray-filled square with black outline, ref 21; $\square$, ref 22; gray asterisk, ref 23; gray plus, ref 24; *, refs 25 and 27; $\times$, ref 26; dark gray-filled square with black outline, ref 28; gray-filled diamond with black outline, ref 29; $\diamond$, ref 30; gray-filled circle with black outline, ref 31; $\blacksquare$, ref 32; gray-filled circle, ref 33. The recommendations of Maryott and Smith[34] are not shown in Figure 1 because they are coincident with the values reported by Tangl.[14]

for formation evaluation. Thus, there is a need to measure the relative electric permittivity at frequencies between 10 Hz and 3 GHz at temperatures up to about 400 K and pressures below 100 MPa with an uncertainty of about 0.1 %.

We now return to describe the measurements of relative electric permittivity at temperature and pressure.

Recent work has demonstrated measurements of viscosity with a vibrating wire[10] and the use of a radio frequency re-entrant cavity operating at frequencies between (220 and 340) MHz for the detection of dew temperatures[11] and the determination of relative permittivity and density within the gas phase and liquid volume fraction formed within the two-phase region for $(0.4026\ CH_4 + 0.5974\ C_3H_8)$.[12] In ref 12, gas phase relative permittivities between (1.05 and 1.17) were determined with an uncertainty of 0.01 %.

In this article, measurements of the relative electric permittivity of liquid methylbenzene are reported from measurements of the resonance frequency of the radio frequency re-entrant cavity. These measurements were intended to validate the anticipated expanded uncertainty in ϵ' by comparison of the results reported with those documented by others with experimental techniques that utilize different principles and have quite different sources of systematic error. However, as Figure 1 shows, even at $p = 0.1$ MPa, the literature values of ϵ' vary by about 4 %;[13–33] the measurements reported in refs 20 to 22 are at pressures below 407 MPa. The recommendations of Maryott and Smith[34] are not shown in Figure 1 because they are coincident with the values reported by Tangl.[14] Consequently, the relative permittivity reported for methylbenzene, which is an industrially important fluid, contributes to the databases of the thermophysical properties for these fluids.

A method of determining the complex relative electric permittivity with an uncertainty of < 0.1 % at frequencies on the order of between (1 and 10^9) Hz is also required at

temperatures up to 473 K and pressures of 200 MPa with corrosive materials. This frequency range requires at the lower frequency range $\approx$ (1 to 10^6) Hz impedance measurements be used, while over the frequency range $\approx$ (10^6 to 10^9), reflection coefficients are determined with network analyzers. These requirements place robustness as a superior priority to accuracy that is of secondary importance provided it is known: the instrument is "fit-for-purpose".[35] Techniques for the measurement of relative electric permittivity, including refractive index, for both electrically conducting fluids and insulators, have been discussed by Moldover et al.[36] Based on the information in ref 36, for this application a guarded parallel plate capacitor would suffice while a guarded concentric cylinder capacitor is preferred. A coaxial cylinder has been used for measurements with petroleum substances when operated at frequencies between (10^3 and 10^9) Hz.[37] In general, devices fabricated by the methods of MicroElectroMechanical Systems (MEMS) are suited to the requirements found in the petroleum industry,[38,39] and SiO_2 has been used to form stable capacitors for use as transportable laboratory standards[40] that might be calibrated with calculable capacitors[41–43] (an electron counting capacitance standard that utilizes a single-electron tunneling device and the definition of capacitance have been described by Keller et al.[44] and Zimmerman et al.[45]). However, the MEMS fabrication process necessarily precludes the use of curved surfaces and requires adoption of a parallel plate capacitor, for which the vacuum capacitance must be stable with respect to time in a thermal cycled environment. Further design constraints are provided by the practical requirement to obtain a capacitance on the order of 1 pF, which permits the measurement of capacitance with sufficient precision with routine electronics, from an object with dimensions on the order of 1 mm. These two constraints require the parallel plate capacitor be formed from interdigitated combs, shown schematically in Figure 2, which is the MEMS design layout, and as a photograph and Scanning Electron Microscope (SEM) image in Figure 3, that is based on the comb actuators.[46–49] Interdigitated comb capacitors have been described as humidity sensors,[50] shear stress sensors,[51] accelerometers,[52] tunable variable capacitors,[53] and vertical comb actuators.[54]

In this article, preliminary measurements of the relative permittivity of methylbenzene will be discussed along with the utility of the comb capacitor, alluded to in ref 39, for the determination of complex relative electric permittivity.

Working Equations

Re-Entrant Cavity. The lumped-parameter (equivalent circuit) model reported by Hamelin et al.[55,56] was used to obtain the complex electric permittivity ϵ_r from the measured resonant frequency f through eq 2 of ref 12. The electrical conductivity of methylbenzene is small, and the resonance quality factor is sufficiently large so terms in Q^{-2} are rendered negligible.[36,56] The real part of the complex quantity $\epsilon_r \equiv \epsilon' - i\epsilon''$, which can depend on frequency, is the dielectric constant ϵ', while the imaginary part, $\epsilon'' = \sigma/(\omega\epsilon_0)$ accounts for electrical dissipation within the dielectric fluid owing to the electrical conductivity σ. Equation 2 of ref 12 was derived assuming both σ and ϵ' are independent of frequency. When $\sigma << 1$, then $\epsilon'/\epsilon'' >> 1$, and simple measurements of frequency suffice because $\mathcal{R}(\epsilon_r) \equiv \epsilon'$; eq 2 of ref 57 gives the low-loss approximation to eq 2 of ref 12.

According to the zero-order model for the re-entrant resonator (eq 1 of ref 12), the product $\mu_r\epsilon'$ of relative magnetic permeability and ϵ', the relative electric permittivity of the fluid, along with the inductance and capacitance under vacuum determine
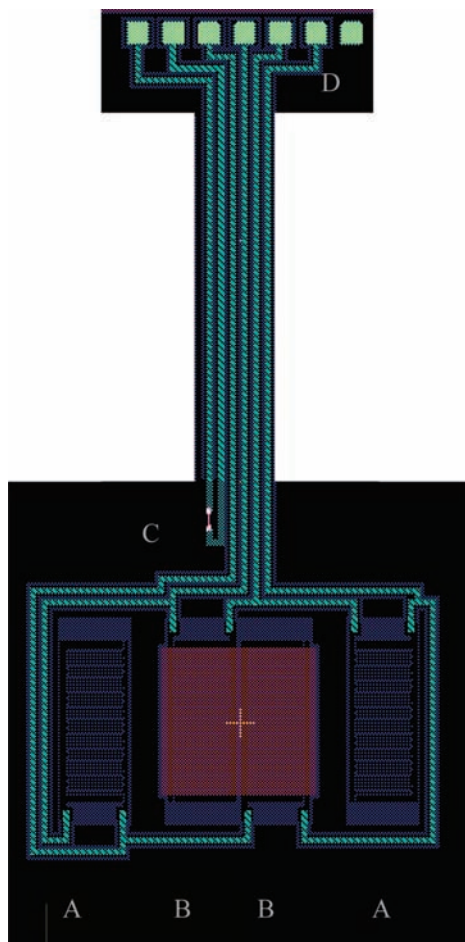
Figure 2. Schematic of the interdigitated comb capacitor fabricated by the techniques of MEMS with four capacitors that are interconnected to form a Wheatstone bridge. Two of the capacitors labeled A are exposed to a dielectric of silicon, while the other two labeled B are exposed to the fluid. The capacitors A and B are interconnected to form a Wheatstone bridge and, along with a boron-doped polycrystalline silicon resistor C capable of operating as a thermometer connected by aluminum, illustrated with turquoise, to wire-pond pads D.

the resonance frequency. For methylbenzene, $\sigma << 1$ and $\mathscr{R}(\epsilon_r) \equiv \epsilon'$, so the relative electric permittivity of the fluid is well approximated by ϵ' and the assumption μ_r is invariant results in a negligible additional uncertainty.[36]

To obtain ϵ', all products, $L_i C_i$, of the cavity must be accounted for including fringing fields, induction effects for the capacitors, capacitive effects for the inductors, and contribution from the 5 mm gap at the bottom of the cavity. The capacitances associated with fringing fields at the ends of the capacitive section were estimated with the methods described by Marcu-witz.[58]

MEMS. The capacitance for one of the fluid capacitors C_{AB} (labeled B in Figure 2 and Figure 3) that is part of the Wheatstone bridge circuit, shown in Figure 4, is given by

$$C_{AB} = C_1 + \{C_2^{-1} + [(C_3^{-1} + C_4^{-1})^{-1} + (C_5^{-1} + C_6^{-1} + C_7^{-1})^{-1}]^{-1}\}^{-1} \quad (1)$$

where the subscripts refer to the capacitances of Figure 4. The space between the interdigitated prongs of the capacitors C_2 and C_4 is filled with silicon that has a relative permittivity of $\epsilon'(\text{Si}) = (11.21 \pm 0.28)$.[59] This value differs by 0.5 from that of (11.7 ± 0.2) reported by Dunlap and Watters but is within 1.02 times the combined uncertainty.[60] A segment of one
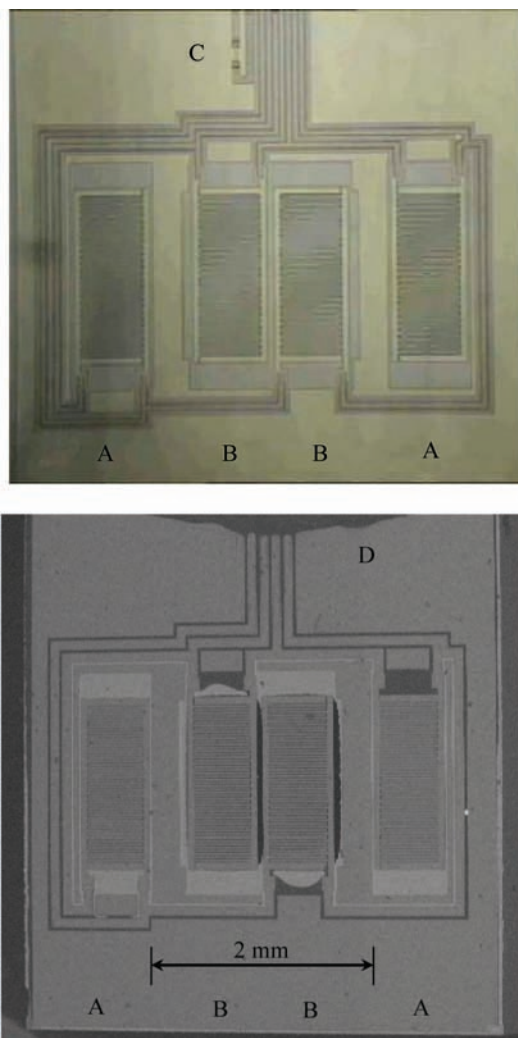

Figure 3. Interdigitated comb capacitor fabricated by the techniques of MEMS with four capacitors that are interconnected to form a Wheatstone bridge. Two of the capacitors labeled A are exposed to a dielectric of silicon, while the other two labeled B are exposed to the fluid. Top: picture of a MEMS capacitor illustrating a boron-doped polycrystalline silicon resistor C capable of operating as a thermometer. Bottom: image obtained from a Scanning Electron Microscope operated with a magnification of 14 of a MEMS packaged as described in ref 39 illustrating the adhesive D used to act as a pressure seal between a stainless steel tube and the printed circuit board.

capacitor (formed from two interdigitated combs) is shown in Figure 5, and the capacitances C_1 ($\equiv C_3$) and C_2 ($\equiv C_4$) in eq 1 are given by

$$C_1 = (n - 1)\epsilon_0 \epsilon' A/d \quad (2)$$

$$C_2 = (n - 1)\epsilon_0 \epsilon'(\text{Si})A/d \quad (3)$$

while C_5 ($\equiv C_7$) and C_6

$$C_5 = \epsilon_0 \epsilon' A/d \quad (4)$$

$$C_6 = \epsilon_0 \epsilon'(\text{Si})A/d \quad (5)$$

In eqs 2 and 3, the number of parallel plate capacitors $n = 49$ and the dimensions in Figure 5 are as follows: the thickness (not shown in Figure 5) $t \approx x \approx 20 \cdot 10^{-6}$ m, $l \approx 5 \cdot 10^{-4}$ m, and thus $A \approx 1 \cdot 10^{-8}$ m^2 and $d \approx 20 \cdot 10^{-6}$ m. With $\epsilon_0 = 8.854\,187\,817 \cdot 10^{-12}$ F·m^{-1}, these values give $C_1 = 0.2196$ pF and $C_2 = 2.462$ pF. For eqs 4 and 5, the dimensions of Figure 5 are: $w \approx 9 \cdot 10^{-4}$ m, $A = 1 \cdot 8 \cdot 10^{-8}$ m^2, and $v \approx z \approx$
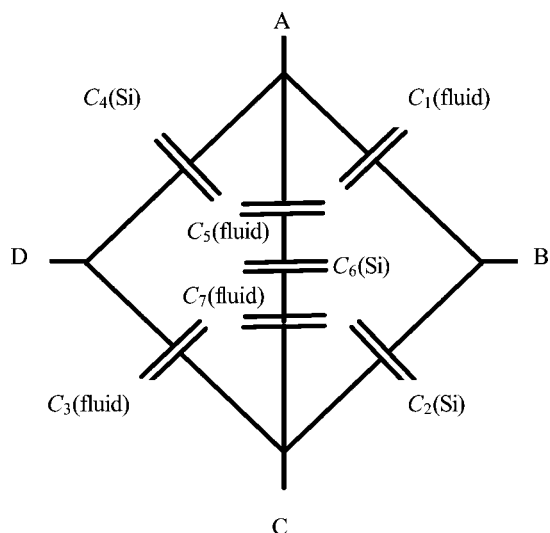
Figure 4. Schematic representation of the Wheatstone bridge configuration of the four capacitances C_n with $n = 1, 2, 3$, and 4 labeled A and B in Figure 3 along with connections A through D and additional contributions arising from the separation of the two fluid exposed capacitors.
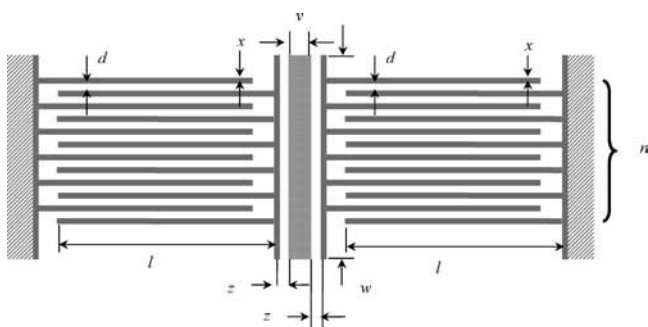

Figure 5. Schematic of the capacitors labeled B in Figure 3 defining the dimensions used in eqs 2 to 5.

$20 \cdot 10^{-6}$ m. $\epsilon'(\text{Si}) = 11.2$ gives $C_5 \approx 0.00797$ pF and $C_6 \approx 0.0893$ pF. With these values, the capacitance C_{AB} (calcd, $p = 0$) of eq 1 is estimated to be 2.8714 pF. Chen et al.[61] have provided similar models for the capacitance of both ground and ungrounded comb-finger capacitors.

Equation 2 must also include a fringing field capacitance. This can be estimated for a parallel plate capacitor with

$$C \approx \frac{\epsilon' \epsilon_0 l}{2\pi} \ln\left(\frac{\pi l}{d}\right) \qquad (6)$$

provided $d \ll l$.[62,63] In eq 6, d is the distance between the plates and l the length and width of the plate. In this work $\epsilon' \approx 2$, $l = 0.5$ mm, and $d = 20 \cdot 10^{-6}$ m, so the fringing field capacitance for each parallel plate in a vacuum is about 0.031 pF. Each capacitor A and B is formed from a combination of 48 parallel plate capacitors. So, the total fringing field for each capacitor B of Figure 3 is 0.148 pF, while that of capacitor A of Figure 3 is about 1.5 pF. These fringing field capacitances are about 50 % of either C_1 or C_2 and thus C_{AB}. However, Iskander and Stuchly[64] and Stuchly[65] report that lumped circuit methods of accounting for fringing fields (eq 6) that arise in the measurement of ϵ' provide upper bounds for the effect because the electric field will, relative to the vacuum, concentrate in the media.

Apparatus, Experimental Procedures, and Calibration

Re-Entrant Cavity. The apparatus has been described in detail elsewhere.[11] The apparatus consisted of a re-entrant resonator
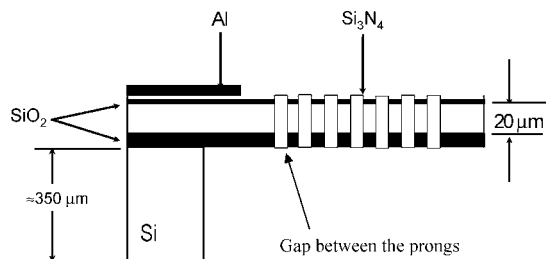

Figure 6. Schematic cross-section through the interdigitated parallel plate comb capacitor fabricated with a $\approx 20 \cdot 10^{-6}$ m thick silicon plate supported on a further $350 \cdot 10^{-6}$ m of silicon. For the sake of clarity, only 7 of the gaps between the interdigitated prongs are shown.

mounted within a circulated air thermostat for which the temperature was controlled to $<\pm 3$ mK. The procedure described in refs 11 and 12 was used to determine the complex resonant frequency $f + ig$, where g is the line-width with a relative standard uncertainty of $\delta f/f \approx 2 \cdot 10^{-7}$. Temperatures were measured with an industrial grade platinum resistance thermometer of nominal resistance 100 Ω that had been calibrated against a standard platinum thermometer of nominal resistance 25 Ω, which itself had been calibrated on ITS-90, with an uncertainty estimated to be 0.02 K. Pressure was generated with a hydraulic pump and measured in the pressure range (5 to 20) MPa, with a dial gauge (Heise, Stratford, CT, model CM12524) with a resolution of 0.1 MPa and a standard uncertainty specified as 0.25 MPa. This uncertainty was confirmed by calibration against a force balance dead weight gauge (Desgranges et Huot model 21000) with an uncertainty of 0.05 MPa.

Dilation of the cavity dimensions resulting from variations in temperature and pressure was accounted for with eq 3 of ref 12 with terms that account for the thermal expansion and dilation. The former is accommodated with the linear thermal expansion coefficient that for a re-entrant resonator constructed from type 316 stainless steel is taken to be $15.9 \cdot 10^{-6}$ K^{-1}.[66] The dilation was accounted for with three parameters γ, f_{00}, and g_{00} that were determined when the cavity was evacuated and filled with methane at six, equally spaced pressures between (3 and 9) MPa on an isotherm at a temperature of 323.15 K that corresponded with a temperature at which Moldover and Buckley[67] reported the relative permittivity of methane determined from capacitance measurements with a toroidal cross capacitor, a technique with entirely different systematic errors than a radio frequency re-entrant cavity. The parameters obtained were reported in ref 11 to be $f_{00} = 344.553$ MHz, $\gamma = 104 \cdot 10^{-6}$ MPa^{-1}, and $g_{00} = 0.585$ MHz. The parameters also account for the variations in spatial distribution of the electromagnetic field within the cavity that occurs between the evacuated and fluid-filled cavity of permittivity greater than the permittivity of free space. This procedure is adopted because the elastic properties are required for a resonator formed from two parts and bolted together. The average absolute differences obtained from the calibration are taken as a measure of the anticipated precision in the measurements and yield an expanded uncertainty in the relative permittivity $\delta\epsilon'/\epsilon' \approx 10^{-4}$.

MEMS Fabrication and Packaging. The MEMS, shown in Figure 2, Figure 3, and Figure 6, was fabricated by École Supérieure d'Ingénieurs en Électrotechnique et Électroniqu (ESIEE) with methods that are similar to those described by Bourouina et al.[68] The complete fabrication process has been described in refs 39 and 69, and only the essential features are provided here. The MEMS was processed on a 101.6 mm diameter silicon-on-insulator wafer (SOI) with crystallographic

plane (1,0,0). It consists of a $20 \cdot 10^{-6}$ m monocrystalline silicon fusion-bonded to a silicon oxide layer (about $0.5 \cdot 10^{-6}$ m thick and called buried oxide or BOX) that isolates the upper layer from the monocrystalline silicon wafer below that has a thickness of about $350 \cdot 10^{-6}$ m. The use of the SOI wafer as the starting material simplifies the deep reactive ion etch used in the micromachining and precisely defines the plate's thickness prior to layer deposition. Atop the $20 \cdot 10^{-6}$ m wafer was deposited about $0.3 \cdot 10^{-6}$ m of silicon dioxide. The silicon was doped, by ion implantation, with boron to adjust the resistance to be less than 1 kΩ and patterned by photolithography to form each prong of the "comb". Silicon nitride, with a stoichiometry similar to Si_3N_4, of thickness of about $0.1 \cdot 10^{-6}$ m was deposited atop the surface coated in etched polysilicon, by low pressure chemical vapor deposition (LPCVD), to form a chemically inert insulating layer. One boron-doped amorphous silicon resistor (labeled C in Figure 2 and Figure 3) could be (but was not in this work) used as the thermometer. A $1 \cdot 10^{-6}$ m thick aluminum layer was deposited by sputtering onto the silicon nitride that, after photolithography, formed metal lines, shown in the cross-section of Figure 6 as well as Figure 2 and Figure 3 with a line width of about $15 \cdot 10^{-6}$ m defining electrical contacts between the capacitors, to form a Wheatstone bridge, resistance thermometer, and wire-bond pads. To protect the transducers from the environment in which they would be immersed, two additional layers were deposited atop the wafer. First, a layer of silicon dioxide about $0.5 \cdot 10^{-6}$ m thick was deposited that was then followed by a layer of protective material that was about $0.6 \cdot 10^{-6}$ m thick. These additional layers underwent photolithography at the wire-bond pads to expose the aluminum so that electrical contacts could be made. Photolithography uses ultraviolet (UV) sensitive material (photoresist) and masks that define shapes, and when this combination is exposed to UV, the resulting patterned surface is chemically etched to remove the unwanted materials deposited onto the wafer to form particular elements. Deep reactive ion etching (DRIE) was then used on the top-face to remove the additional layers and the $20 \cdot 10^{-6}$ m thick silicon between the prongs of the combs to form the capacitors (labeled B in Figure 2 and Figure 3 and illustrated in the cross-section of Figure 6) exposed to the fluid.[70] DRIE was also used to form a gap between both capacitors B. The BOX acted as an etch stop. A second DRIE micromachining step was performed from the back of the chip to remove the underlying 0.350 mm thick silicon beneath the capacitors B as shown in the cross-section of Figure 6. These procedures resulted in combs with 25 prongs, two for each capacitor, that were interdigitated prongs to give 49 parallel plate capacitors in each. Each prong was about 0.5 mm long and $20 \cdot 10^{-6}$ m wide with a thickness, which varied over the surface area, from $(21.6$ to $23) \cdot 10^{-6}$ m with an estimated average thickness of about $22.25 \cdot 10^{-6}$ m. The two capacitors labeled B in Figure 2 and Figure 3 were separated from the substrate at each side and from each other by a gap that was about 0.9 mm long and about $20 \cdot 10^{-6}$ m wide. The other two capacitors (labeled A in Figure 2 and Figure 3 and illustrated in the cross-section of Figure 6), which had the same number of prongs, parallel plates, and gap dimensions, had a dielectric of silicon. In principle, this arrangement permitted the determination of the change in ϵ' of the fluid relative to that of silicon rather than the vacuum. This concept was employed because the environment of intended operation prevents establishing a vacuum. The individual devices on a wafer were separated from each other with a process known as dicing.

The MEMS was mounted on a printed circuit board, and all but the active element were sealed within a tube using adhesive as described in ref 39. It was then placed in a bored-out Swagelock bulkhead connector and connected to both a positive displacement pump and a pressure gauge. The substrate and the metallic container formed the third terminal ground (guard electrode).

The temperature was determined on the International Temperature Scale of 1990 (ITS-90) using a nominal 100 Ω platinum resistance thermometer. The resistance and thus temperature were determined with an ASL F100 with an uncertainty of about 0.01 K. The center of the sensing element was located in the same horizontal plane as the MEMS. The $\delta T = \pm 0.01$ K results in a negligible uncertainty in ϵ' of $\delta|\epsilon'| < 0.00002$ (about 0.001 %) because of the fluids investigated over our temperature and pressure range $|(\partial \epsilon'/\partial T)_p| < 0.002$ K^{-1}.

Pressures were measured using a resonant quartz transducer (Quartzdyne model QHB009-16-200 serial number 157 972 with a maximum operating pressure of 110 MPa and maximum operating temperature of 473 K) with an uncertainty cited by the manufacturer of about 0.02 % of full scale. When the pressure transducer was calibrated against an oil-lubricated dead-weight gauge, it was found to have an uncertainty of $\delta p/\text{MPa} = \{0.0001 \cdot (p/\text{MPa}) + 0.022\}$. The pressure of 0.022 MPa is comparable with the cited uncertainty of the transducer of about 0.02 % for the full-scale pressure of 110 MPa. In the temperature and pressure range investigated, $\delta p < \pm 0.029$ MPa, and when combined, in the worst case, with $(\partial \epsilon'/\partial p)_T \approx 0.002$ MPa^{-1}, corresponds to a potential uncertainty in ϵ' of 0.000058 (or about 0.003 %). The required derivatives with respect to pressure and temperature were determined from literature values described in the Results and Discussion section below. Pressures were generated in the system with an ISCO model 100 DX positive displacement pump with an upper operating pressure of about 68 MPa.

Prior to measurements, the apparatus was evacuated with a turbo-molecular pump, to a pressure (as indicated by an ionization gauge located near the pump) of less than 10^{-2} Pa for at least 24 h. Before filling the apparatus with methylbenzene, the capacitance was measured.

The capacitance was measured with a ratio transformer bridge (Andeen-Hagerling AH2500A opt E) driven at 15 V at a frequency of 1 kHz. This instrument can resolve fractional changes in capacitance $\delta C/C < 10^{-6}$ when C is about 1 pF. The MEMS was connected to the bridge with a pair of coaxial cables, and the ground of each was connected to the metallic body of the MEMS and also the silicon substrate. At the frequency of operation, the impedance of fluid-filled capacitors was sufficiently high to reduce the accuracy of the capacitance measurement by about a factor of 10. At higher frequencies, the output impedance of the transformer increases, and the accuracy of the voltage ratios produced by the transformer is reduced. When the MEMS was immersed in argon, the measured conductance was about 0.1 nS, that is, about 100 times the value expected based on the concentric cylinder capacitors formed from metal. The capacitance $C_{AB}(\text{exptl}, p = 0) = 2.8735$ pF which is 0.07 % above the value estimated from eq 1 of 2.8714 pF.

When the MEMS was immersed in octane, the working eq 1, which excluded the fringing fields, gave values of ϵ' which deviated by -0.7 % at $p = 7$ MPa and 1.4 % at $p = 42$ MPa from the correlation reported by Scaife and Lyons.[71] The differences were a smooth function of pressure, and over the same pressure range ϵ' increased from 1.95 to 1.99. In view of
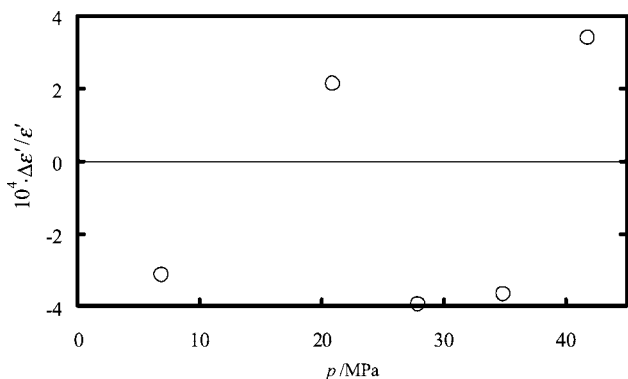
Figure 7. Deviations $\Delta\epsilon' = \epsilon'(\text{exptl}) - \epsilon'(\text{calcd})$ of the measured relative electric permittivity $\epsilon'(\text{exptl})$ of octane determined with eq 7 as deviations from the calculated values $\epsilon'(\text{calcd})$ of ref 71 at pressure p and $T = 297.47$ K.

these differences, we take the agreement between the measured and calculated $C_{AB}(p = 0)$ as fortuitous and place no particular emphasis on it. The differences in ϵ' were accommodated by

$$100 \cdot \Delta\epsilon'/\epsilon' = -8.70697 \cdot 10^{-4}(p/\text{MPa})^2 + 9.91357 \cdot 10^{-2}(p/\text{MPa}) - 1.27334 \quad (7)$$

with a standard deviation of $\pm$ 0.04 %. In view of the assumptions required and the uncertainty in the estimate of the fringing fields, these effects for fluids with $\epsilon' \approx 2$ were accounted for with eq 7 that, as Figure 7 shows, provided ϵ' that differed by about $\pm 4 \cdot 10^{-4}$ from those of ref 71 and is taken as the standard uncertainty of the ϵ' obtained with the MEMS.

Here we digress to comment on the empirical correlation of Scaife and Lyons[71] for the relative electric permittivity of octane that was based on their measurements,[72] obtained with a coaxial cylinder capacitor[73] and deposited as Supporting Information.[74] The fit reported in ref 71 represents the data of ref 74 within $\pm$ 0.15 %. Brazier and Freeman[75] reported measurements of the relative permittivity, not included in ref 71, with an uncertainty of about $\pm$ 0.2 % at $T = 303.15$ K and a pressure below 400 MPa. At pressures between (50 and 250) MPa, the results of ref 75 differ from those of ref 71 by between $-(0.5$ and $0.76)$ %.

Materials. Methylbenzene was obtained from Merck BDH Ltd. (with a stated mass fraction purity of >0.995 and a mass fraction of benzene of 0.002) with a mass fraction, determined by gas chromatography using a flame ionization detector, of >0.9996 with major but unquantified impurities of benzene and water. Prior to use within the re-entrant cavity, the sample was placed for 7 days over grade 0.4 nm molecular sieves that had been previously baked at a temperature of 500 K at a pressure $<10^{-3}$ Pa. A Karl Fischer titration of the methylbenzene gave a water mass fraction of $<1 \cdot 10^{-6}$ g. After use within the re-entrant resonator, the mass fraction purity of the methylbenzene was found to be 0.994 with a retention time on the column of 92 s, and the major impurity was 0.0047 with a retention time of 77 s without chemical identification. Benzene is the most plausible chemical impurity but unlikely due to the absence of exposure of the apparatus to benzene. Owing to both the propensity and difficulty of removing water from metallic surfaces, it is always present but not detectable with a flame ionization detector. Octane was used to determine the fringing field capacitance at a relative permittivity of 1.94756 at $T = 298$ K and $p = 5$ MPa. The octane, supplied by Koch-Light, was puriss grade with a mass fraction purity of 0.99 as determined by glc.

Table 1. Mean Relative Electric Permittivity $\langle\epsilon'\rangle$ of Methylbenzene Obtained from N Measurements of the Resonant Frequency of a Methylbenzene Filled Re-Entrant Cavity at Mean Temperature $\langle T \rangle$ and Pressure $\langle p \rangle$[a]

$\langle T\rangle$/K	$\langle p\rangle$/MPa	N	$\langle\epsilon'\rangle$	$\langle T\rangle$/K	$\langle p\rangle$/MPa	N	$\langle\epsilon'\rangle$
290.63	0.10	6	2.40453	324.54	3.20	6	2.32625
290.65	0.10	5	2.40448	324.54	6.31	6	2.33179
290.69	2.17	3	2.41272	324.58	8.37	6	2.33528
290.77	4.24	5	2.41409	324.61	12.51	6	2.34222
290.81	6.31	3	2.41721	324.62	16.65	6	2.34897
290.83	8.37	4	2.42020	339.31	0.10	6	2.28784
290.87	12.51	6	2.42629	339.35	2.17	6	2.29190
290.88	16.10	3	2.43136	339.38	4.24	6	2.29596
290.90	16.65	6	2.43220	339.38	6.31	6	2.29992
291.15	0.10	6	2.39830	339.39	8.37	6	2.30380
292.65	0.10	5	2.40346	339.41	16.65	6	2.31844
294.80	0.10	6	2.39092	339.41	12.51	6	2.31127
310.68	0.10	6	2.35675	357.44	6.31	6	2.26156
310.79	0.10	7	2.35646	357.45	4.24	6	2.25717
311.94	0.10	6	2.35363	357.45	2.17	6	2.25261
314.47	0.10	7	2.34790	357.46	0.10	7	2.24793
315.68	0.10	5	2.34035	357.52	8.37	6	2.26578
315.77	0.10	6	2.33999	357.54	12.51	6	2.27400
315.78	8.37	6	2.35428	357.55	16.65	6	2.28185
315.78	1.14	6	2.34185	390.53	0.17	10	2.17781
315.79	4.24	6	2.34729	390.53	2.17	9	2.18342
315.79	2.17	6	2.34366	390.59	4.24	8	2.18899
315.79	3.20	6	2.34545	390.59	0.10	8	2.17698
315.79	12.51	6	2.36095	390.61	6.31	7	2.19431
315.79	16.65	6	2.36740	390.63	8.37	8	2.19969
315.79	19.41	5	2.37152	390.65	12.51	9	2.20969
315.79	6.31	6	2.35078	390.68	16.65	11	2.21925
320.64	0.10	6	2.32926	405.84	2.17	8	2.14947
320.66	1.14	6	2.33114	406.30	6.31	6	2.16081
324.50	0.10	6	2.32053	406.32	4.24	6	2.15467
324.53	1.14	6	2.32241	406.37	8.37	10	2.16653
324.54	2.17	6	2.32435	406.54	12.51	6	2.17721
324.54	4.24	6	2.32811	406.64	16.65	6	2.18731

[a] The expanded ($k = 2$) uncertainties of the measurements are: $\delta T = 0.02$ K, $\delta p = 0.01$ MPa, and $\delta\epsilon' = 0.0002$.

Results and Discussion

The ϵ' values for methylbenzene obtained with the re-entrant cavity are listed in Table 1. The estimated expanded ($k = 2$) uncertainty of the ϵ' obtained with the re-entrant cavity of $\delta\epsilon' = 0.0003$ was obtained from the calibration measurements with methane and the uncertainty of the resonance frequency measurements.

There are numerous models, some with theoretical basis, which have been used to represent the relative permittivity as a function of density, and for polar fluids, these expressions that correlate the total molar polarizability have been discussed by Böttcher.[76] One of these expressions is the equation of Kirkwood and Onsager,[77] and another adopted by Eltringham and Catchpole[78] is an adaptation of the Clausius–Mossotti equation.[79] For measurements of ϵ' as a function of temperature and pressure, an alternative empirical expression was reported by Owen and Brinkley.[80] This equation was analogous to the Tait equation[81] for density and accommodated the pressure dependence of the dielectric constant. It can be written in the form

$$\epsilon'(T,p) = \frac{\epsilon'(T,p_r)}{1 - C\lg\{(B(T)+p)/(B(T)-p_r)\}} \quad (8)$$

where $B(T)$ is an empirical function of temperature T and $\epsilon'(T, p_r)$ dependent on both temperature and the reference pressure p_r. Equation 8 is consistent with Tammann's hypothesis[82] and electrostatics. Skinner et al.,[20] based on Kirkwoods[83] equation, suggest that C of eq 8 is greater than the analogous coefficient

Table 2. Relative Electric Permittivity ϵ' of Methylbenzene Obtained with the MEMS at Temperature T and Pressure p^a

T/K	p/MPa	ϵ'
297.41	6.919	2.3777
297.40	13.927	2.3962
297.39	20.942	2.4127
297.38	27.906	2.4276
297.37	34.905	2.4430
297.37	41.879	2.4564

^{a} The expanded ($k = 2$) uncertainties of the measurements are $\delta T = 0.02$ K, $\delta p = 0.002$ MPa, and $\delta\epsilon' = 0.002$.

of the Tait equation. In eq 8, $p_r = 0.1$ MPa and $\epsilon'(T, p_r)$ listed in Table 2 were represented by

$$\epsilon'(T, p_r) = \sum_{i=0}^{1} A_i (T/K)^i \qquad (9)$$

with a standard deviation of the mean $\sigma(<\epsilon'>)$ that gives $100 \cdot s(<\epsilon'>)/\epsilon' = \pm 0.29$ when the parameters were $A_0 = 3.066917$ and $A_1 = -0.00229$. The $\epsilon'(p_r)$ values obtained from eq 9 were combined with the ϵ' of Table 1 to determine the adjustable parameter C of eq 8 and the coefficients of

$$B(T) = \sum_{i=0}^{2} b_i (T/K)^i \qquad (10)$$

with the results $b_0 = -153.201$ MPa, $b_1 = 1.262$ MPa, $b_2 = -0.00210$ MPa, and $C = 0.0304$ that represented the data with $100 \cdot s(<\epsilon'>)/\epsilon' = \pm 0.33$ that is about 10 times the estimated uncertainty in an individual measurement of ϵ'.

Comparison with Literature Data. The $\epsilon'(p = 0.1$ MPa) reported by other works[13—33] are shown as deviations from eqs 8 to 10 and the smoothing equation in Figure 8. In the overlapping temperature range, the values reported by Lewis and Smyth[18] and Mospik[22] agree with those of Table 1, while those of refs 13, 25, 27, and 29 are all systematically below those obtained from the re-entrant cavity by about 2 %, that is, about 7 times the combined uncertainties.

The ϵ' values determined with the MEMS and listed in Table 2 have an estimated expanded uncertainty of $\delta\epsilon' = \pm 0.001$ that includes the most significant source of error that arises from calibration. These values were extrapolated, with an equation quadratic in pressure that represented the data with a standard deviation of 0.0002, to $p = 0.1$ MPa and, as Figure 8 shows, differs from eq 9 by -1 %, that is, within 5 times the combined uncertainty obtained of our measurements at a confidence interval of 0.995. This agreement is considered remarkable because of the magnitude of the fringing field capacitances and the observed differences between the literature values shown in Figure 1.

The ϵ' values listed in Table 1 are shown as a function of p in Figure 9 and Figure 10 as relative deviations from eqs 8 to 10. The data from Table 1 are shown in Figure 9 and at $T \leq 357$ K lie within the standard deviation of the fit, while those at $T = (390$ and $406)$ K exhibit differences between (0.2 and 1) % that increase with increasing pressure that, while systematic, are within 3 times the standard deviation of the fit and about 10 times the uncertainty in an individual measurement.

To seek an explanation for these differences, we assume the measurements at $T \leq 357$ K are for all intents and purposes exact, and then we can speculate that the relative deviations shown in Figure 9 might arise from one or more of the following plausible sources of error: (1) the assumption that the linear thermal expansion coefficient of stainless steel is a constant over
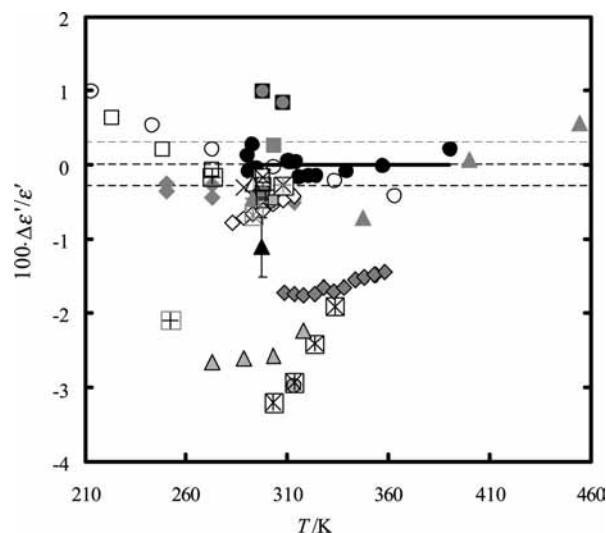

Figure 8. Deviations $\Delta\epsilon' = \epsilon'(\text{exptl}) - \epsilon'(\text{calcd})$ of the measured relative electric permittivity $\epsilon'(\text{exptl})$ of methylbenzene as deviations from the calculated values $\epsilon'(\text{calcd})$ of eq 9 at $p = 0.1$ MPa. At $T \geq 383.75$ K, the normal boiling temperature, measurements were performed at $p > p^{l+g}$ where p^{l+g} is the vapor pressure. Gray-filled triangle with black outline, ref 13; gray-filled and outlined triangle, ref 14; gray cross, ref 15; gray diamond, ref 16; $\triangle$, ref 17; $\bigcirc$, ref 18; $+$, ref 19; gray-filled square, ref 20; light gray-filled square with black outline, ref 21; $\square$, ref 22; gray asterisk, ref 23; gray plus, ref 24; *, refs 25 and 27; $\times$, ref 26; dark gray-filled square with black outline, ref 28; gray-filled diamond with black outline, ref 29; $\diamond$, ref 30; gray-filled circle with black outline, ref 31; $\blacksquare$, ref 32; gray-filled circle, ref 33; $\blacktriangle$, MEMS obtained by extrapolation of the results listed in Table 2 with a quadratic function of pressure to $p = 0.1$ MPa. The recommendations of Maryott and Smith[34] are not shown in Figure 1 because they are coincident with the values reported by Tangl.[14] The dashed lines at ± 0.3 are $100 \cdot s(<\epsilon'>)/\epsilon' = \pm 0.29$ where s is the standard deviation of the fit to eq 9 while that at 0 indicates an extrapolation of eq 9.
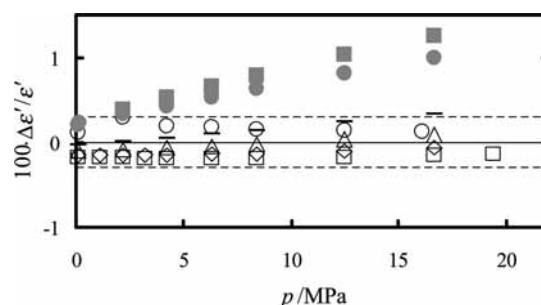

Figure 9. Deviations $\Delta\epsilon' = \epsilon'(\text{exptl}) - \epsilon'(\text{calcd})$ of the measured relative electric permittivity $\epsilon'(\text{exptl})$ of methylbenzene listed in Table 1 as deviations from the calculated values $\epsilon'(\text{calcd})$ of eqs 8 to 10 at pressure p. $\bigcirc$, $T = 290$ K; $\square$, $T = 315$ K; $\diamond$, $T = 325$ K; $\triangle$, $T = 339$ K; $-$, $T = 357$ K; gray-filled circle, $T = 390$ K; and gray-filled square, $T = 406$ K. The dashed lines are $100 \cdot s(<\epsilon'>)/\epsilon' = \pm 0.33$ where s is the standard deviation of the fit to eqs 8 to 10.

a temperature range of 67 K; (2) the calibration for dilation was performed solely at one temperature that in effect assumes the elastic constants are independent of temperature over a range of 50 K; and (3) a variation of the mole fraction of water for which $\epsilon'(293$ K$) \approx 80$. The variations shown in Figure 9 negate item 3 as a possible cause owing to the reproducibility of the differences with respect to pressure at different temperatures. The linear thermal expansion coefficient varies insignificantly over the temperature range of interest for the determination of capacitance from the measured resonance frequency, rendering negligible the differences that arise from item 1. However, the deviations shown in Figure 9 increase linearly with increasing pressure and tend to 0 as $p \rightarrow 0$ which is consistent with an
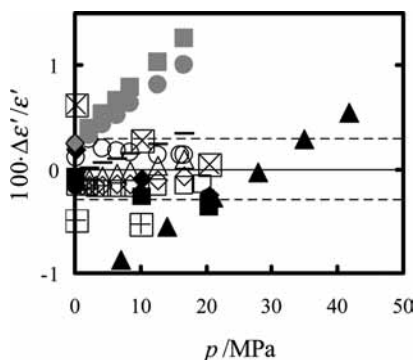
Figure 10. Deviations $\Delta\epsilon' = \epsilon'(\text{exptl}) - \epsilon'(\text{calcd})$ of the measured relative electric permittivity $\epsilon'(\text{exptl})$ of methylbenzene listed in Table 1 and Table 2 as deviations from the calculated values $\epsilon'(\text{calcd})$ of eqs 8 to 10 at pressure p. $\bigcirc$, $T = 290$ K; $\square$, $T = 315$ K; $\Diamond$, $T = 325$ K; $\triangle$, $T = 339$ K; $-$, $T = 357$ K; gray-filled circle, $T = 390$ K; gray-filled square, $T = 406$ K; $\blacktriangle$, MEMS data, $T = 297$ K; gray-filled diamond with black outline, $T = 303.15$ K, ref 20; $\times$, $T = 223$ K, ref 22; $\blacklozenge$, $T = 248$ K, ref 22; $\blacksquare$, $T = 273$ K, ref 22; $\bullet$, $T = 298$ K, ref 22. The dashed lines are $100 \cdot s(<\epsilon'>)/\epsilon' = \pm 0.33$ where s is the standard deviation of the fit to eqs 8 to 10.

uncertainty in the coefficients of the expression to accommodate dilation. Young's modulus E decreases with increasing temperature, and for stainless steel $(1/E) \cdot dE/dT \approx -0.02$ K^{-1}.[84] Our assumption of $(1/E) \cdot dE/dT = 0$ results in an overestimate of the effect of dilation on the resonance frequency, and consequently, the apparent capacitance and relative electric permittivity will be systematically high. Based solely on these comparisons, we conclude the differences shown in Figure 9 arise from our assumptions accommodating dilation. Neither experiments nor detailed calculations have been performed to confirm this conjecture.

The $\epsilon'(p)$ values of Table 2 are shown with the measurements reported in refs 20 and 21 in Figure 10 but limited to pressures up to $p = 50$ MPa. The values obtained with the MEMS deviate systematically from eqs 8 to 10 with differences that increase with increasing pressure from -1 % at $p = 7$ MPa to 0.5 % at $p = 42$ MPa which represents an extrapolation of eq 8 by a factor of 2 in pressure. In the overlapping pressure range, the measurements reported by Mospek[21] even at temperatures 67 K below the lowest of Table 1 lie within ± 0.3 % of our results. The values of ref 20, which extend to pressures of 400 MPa, differ from eqs 8 to 10 with differences that increase with increasing pressure from 0.3 % at $p = 0.1$ MPa to 6 % at $p = 407$ MPa; only the measurement at $p = 0.1$ MPa can be shown on the abscissa of Figure 10.

Conclusions

The values of ϵ' determined at $T \leq 357$ K with the re-entrant cavity agree with those from the literature obtained from experimental techniques that utilize different principles and thus have quite different sources of systematic error, within a reasonable multiple of the estimated uncertainty. At $T = (390$ and 406$)$ K, assuming the literature data are reliable, the results exhibit an, as of yet, unexplained, systematic deviation that may arise from the calibration, performed at $T = 323$ K to account for the dilation of the cavity dimensions with respect to pressure.

The MEMS device for the measurement of relative electric permittivity had four capacitors. Two were exposed to fluid and two to silicon. Each was fabricated from 49 parallel plate capacitors formed from interdigitated prongs (comb). Not surprisingly, this arrangement had fringing field capacitances (which depend on ϵ') that contributed about 50 % to the capacitance. The four capacitors were interconnected to form a

Wheatstone bridge, and the capacitance was dominated by the $\epsilon'(\text{Si}) \approx 11$. These two artifacts rendered the measurement of ϵ' unviable without recourse to a calibration with a fluid for which ϵ' is about that of the unknown to be measured; in this case of methylbenzene of about 2. In view of this restriction, no attempt was made to determine the response of the device over a temperature and pressure range experienced in petroleum reservoirs. Nevertheless, the uncertainty of the measurement, when calibrated, is sufficient to distinguish the differences in ϵ' between conventional oil ($\epsilon' \approx 2$) and heavy oil ($\epsilon' \approx 3$).

Literature Cited

(1) Meyer R. F.; Attanasi, E. *Natural Bitumen and Extra Heavy Oil, 2004 Survey of Energy Resources*p; Trinnaman, J., Clarke, A., Eds. for the World Energy Council; Elsevier: Amsterdam, 2004; Chapter 4, p 93–117..

(2) Tao, R.; Xu, X. Reducing the Viscosity of Crude Oil by Pulsed Electric or Magnetic Field. *Energy Fuels* **2006**, *20*, 2046–2051.

(3) Goual, L; Firoozabadi, A. Measuring Asphaltenes and Resins, and Dipole Moment in Petroleum Fluids. *AIChE J.* **2002**, *48*, 2646–2663.

(4) Sen, A. D.; Anicich, V. G.; Arakelian, T. Dielectric Constant of Liquid Alkanes and Hydrocarbon Mixtures. *J. Phys. D: Appl. Phys.* **1992**, *25*, 516–521.

(5) Abernethy, E. R. Production Increase Of Heavy Oils By Electromagnetic Heating. *J. Can. Pet. Technol.* **1976**, *12*, 91–97.

(6) Sresty, G. C.; Dev, H.; Snow, R. H.; Bridges, J. E. Recovery of Bitumen from Tar Sand Deposits with the Radio Frequency Process. *Soc. Pet. Eng.* 10229.

(7) Fanchi, J. R. Feasibility of Reservoir Heating by Electromagnetic Irradiation. *Soc. Pet. Eng.* 20483

(8) Ovalles, C.; Fonseca, A.; Lara, A.; Alvarado, V.; Urrecheaga, K.; Ranson, A.; Mendoza, H. Opportunities Of Downhole Dielectric Heating In Venezuela: Three Case Studies Involving Medium Heavy and Extra Heavy Crude Oil Reservoirs. *Soc. Pet. Eng.* 78980

(9) Kasevich, R. S.; Price, S. L.; Faust, D. L.; Fontaine, M. F. Pilot testing of a radio frequency heating system for enhanced oil recovery from diatomaceous earth. *Soc. Pet. Eng.* 28619

(10) Kandil, M.; Marsh, K. N.; Goodwin, A. R. H. A Vibrating Wire Viscometer with Wire Diameters of (0.05 and 0.15) mm: Results for Methylbenzene and two Fluids with Nominal Viscosities at $T = 298$ K and $p = 0.01$ MPa of (14 and 240) mPa·s at Temperatures between (298 and 373) K and Pressures below 40 MPa. *J. Chem. Eng. Data* **2005**, *50*, 647–655.

(11) Kandil, M. E.; Marsh, K. N.; Goodwin, A. R. H. A re-entrant resonator for the measurement of phase boundaries: dew points for {0.4026CH4 + 0.5974C3H8}. *J. Chem. Thermodyn.* **2005**, *37*, 684–691.

(12) Kandil, M.; Marsh, K. N.; Goodwin, A. R. H. Determination of the relative permittivity and density within the gas phase and liquid volume fraction within the two phase region for (0.4026 CH$_4$ + 0.5974 C$_3$H$_8$) with a radio frequency re-entrant cavity. *J. Chem. Eng. Data* **2007**, *52*, 1660–1671.

(13) Ratz, F. Dependence of the dielectric constant on temperature and pressure. *Z. Phys. Chem.* **1896**, *19*, 94–112.

(14) Tangl, K. Alteration of the dielectric constant of some liquids with temperature. *Ann. Phys.-Berlin* **1903**, *10*, 748–67.

(15) Williams, J. W.; Krchma, I. J. The dielectric constants of binary mixtures. *J. Am. Chem. Soc.* **1926**, *48*, 1888–1896.

(16) Cowley, E. G.; Parrington, J. R. Studies in dielectric polarisation. Part XXI. The effect of solvent and temperature upon the polarisation and apparent moments of bromides. *J. Chem. Soc.* **1937**, 130–138.

(17) Müller, F. H. The dipole moment of chlorobenzene and the solvent effect of thirty-four different liquids. *Physik. Z.* **1937**, *38*, 283–292.

(18) Lewis, G. L.; Smyth, C. P. Internal Rotation and Dipole Moment in Succinonitrile. *J. Chem. Phys.* **1939**, *7*, 1085–1093.

(19) Guillien, R. J. The dielectric constand in the neighborhold of the fusion point. *Phys. Radium* **1940**, *1*, 29–33.

(20) Skinner, J. L.; Cussler, E. L.; Fuoss, R. M. Pressure dependence of dielectric constant and density of liquids. *J. Phys. Chem.* **1968**, *72*, 1057–1064.

(21) Hartmann, H.; Schmidt, A. P. Effect of pressure on the static dielectric constants of liquids at 30 and 50 deg. *Ber. Bunsen. Phys. Chem.* **1968**, *72*, 875–877.

(22) Mopsik, F. I. Dielectric properties of slightly polar organic liquids as a function of pressure, volume and temperature. *J. Chem. Phys.* **1969**, *50*, 2559–2569.

(23) Dhillon, M. S.; Chugh, H. S. Dielectric Constants and Molar Polarizations of 1,2-Dibromoethane in Cyclohexane, Benzene, Methylbenzene, 1,2-Dimethylbenzene, 1,3-Dimethylbenzene, and 1,4-Dimethylbenzene at 303.15 K. *J. Chem. Eng. Data* **1978**, *23*, 263–265.

(24) Nath, J.; Tripathi, A. D. Binary Systems of 1,1,2,2-Tetrachloroethane with Benzene, Toluene, p-Xylene, Acetone and Cyclohexane. *J. Chem. Soc., Faraday Trans. 1* **1984**, *80*, 1517–1524.

(25) Singh, R. P.; Sinha, C. P. Dielectric Behavior of Ternary Mixtures of Toluene, Chlorobenzene, I-Hexanol, and Benzyl Alcohol. *J. Chem. Eng. Data* **1985**, *30*, 474–476.

(26) Ritzoulis, G.; Papadopoulos, N.; Jannakoudakis, D. Densities, Viscosities, and Dielectric Constants of Acetonitrile + Toluene at 15, 25, and 35 °C. *J. Chem. Eng. Data* **1986**, *31*, 146–148.

(27) Singh, R. P.; Sinha, C. P.; Singh, B. N. Dielectric Behavior of the Ternary Systems of Toluene, Chlorobenzene, and I-Hexanol with n-Hexane-Benzyl Atcohol as Their Partially Miscible Binary Subsystem. *J. Chem. Eng. Data* **1986**, *31*, 112–115.

(28) Buep, A. H.; Barón, M. Dielectric Properties of Binary Systems. 7. Carbon Tetrachloride with Benzene, with Toluene, and with p-Xylene at 298.15 and 308.15 K. *J. Phys. Chem.* **1988**, *92*, 840–843.

(29) Mardolcar, U. V.; Nieto de Castro, C. A.; Santos, F. J. V. Dielectric constant measurements of toluene and benzene. *Fluid Phase Equilib.* **1992**, *79*, 255–264.

(30) Moumouzias, G.; Ritzoulis, G. Relative Permitivities and Refractive Indices of Propylene Carbonate + Toluene Mixtures from 283.15 to 313.15 K. *J. Chem. Eng. Data* **1997**, *42*, 710–713.

(31) Fornefeld-Schwarz, U. M.; Svejda, P. Refractive Indices and Relative Permittivities of Liquid Mixtures of γ-Butyrolactone, γ-Valerolactone, δ-Valerolactone, or ϵ-Caprolactone + Benzene, + Toluene, or + Ethylbenzene at 293.15 and 313.15 K and Atmospheric pressure. *J. Chem. Eng. Data* **1999**, *44*, 597–604.

(32) Sastry, N. V.; Valand, M. K. Volumetric Behaviour of Alkyl Acrylates-1-Alcohols at 298.15 and 308.15 K. *Phys. Chem. Liq.* **2000**, *38*, 61–72.

(33) George, J.; Sastry, N. V. Densities, Excess Molar Volumes at T = (298.15 to 313.15) K, Speeds of Sound, Excess Isentropic Compressibilities, Relative Permittivities, and Deviations in Molar Polarizations at T = (298.15 and 308.15) K for Methyl Methacrylate + 2-Butoxyethanol or Dibutyl Ether + Benzene, Toluene, or p-Xylene. *J. Chem. Eng. Data* **2004**, *49*, 1116–1126.

(34) Maryott, A. A.; Smith, E. R. Table of Dielectric Constants of Pure Liquids. Natl. Bur. Stand. Circ. 514, August 10, 1951.

(35) Wakeham, W. A.; Assael, M. A.; Atkinson, J. S.; Bilek, J.; Fareleira, J. M. N. A.; Fitt, A. D.; Goodwin, A. R. H.; Oliveira, C. M. B. P. Thermophysical Property Measurements: The Journey from Accuracy to Fitness for Purpose. *Int. J. Thermophys.* **2007**, *28*, 372–416.

(36) Moldover, M. R.; Marsh, K. N.; Barthel, J.; Buchner, R. Relative Permittivity and Refractive Index. In *Experimental Thermodynamics Vol. VI, Measurement of the Thermodynamic Properties of Single Phases*; Goodwin, A. R. H., Marsh, K. N., Wakeham, W. A., Eds. for International Union of Pure and Applied Chemistry; Elsevier: Amsterdam, 2003; Chapter 9, pp 127–235.

(37) Folgerø, K.; Frjisø, T.; Hilland, J.; Tjomsland, T. A broad-band and high sensitivity dielectric spectroscopy measurement system for quality determination of low-permeability fluids. *Meas. Sci. Technol.* **1995**, *6*, 995–1008.

(38) Werner, M. R.; Fahrner, W. R. Review on Materials, Microsensors, Systems, and Devices for High-Temperature and Harsh-Environment Applications. *IEEE Trans. Ind. Elec.* **2001**, *48*, 249–257.

(39) Goodwin, A. R. H.; Donzier, E. P.; Vancauwenberghe, O.; Manrique de Lara, M.; Marty, F.; Mercier, B.; Fitt, A. D.; Ronaldson, K. A.; Wakeham, W. A. A Vibrating Edge Supported Plate, Fabricated by the Methods of Micro Electro Mechanical System (MEMS), for the Simultaneous Measurement of Density and Viscosity: Results for Methylbenzene and Octane at Temperatures between (323 and 423) K and Pressures in the range (0.1 to 68) MPa. *J. Chem. Eng. Data* **2006**, *51*, 190–208.

(40) Cutkosky, R. D.; Lee, L. H. Improved Ten-Picofarad Fused Silica Dielectric Capacitor. *J. Res. Natl. Bur. Stand.* **1965**, *69C*, 173–179.

(41) Cutkosky, R. D. Evaluation of the NBS unit of resistance based on a calculable capacitor. *J. Res. Natl. Bur. Stand.* **1961**, *65A*, 147–158.

(42) Elnquist, R. E.; Cage, M. E.; Tang, Y.-H.; Jeffery, A.-M.; Kinard, J. R., Jr.; Dziuba, R. F.; Oldham, N. M.; Williams, E. R. The Ampere and Electrical Standards. *J. Res. Natl. Inst. Stand. Technol.* **2001**, *106*, 65–103.

(43) Shields, R. L.; Field, B. F.; Layer, H. P. New realization of the ohm and farad using the NBS calculable capacitor. *IEEE Trans. Instrum. Meas.* **1989**, *38*, 249–251.

(44) Keller, M. A.; Eichemberger, A. L.; Martinis, J. M.; Zimmerman, N. M. A Capacitance Standard Based on Counting Electrons. *Science* **1999**, *285*, 1706–1709.

(45) Zimmerman, N. M.; El Sabbagh, M. A.; Wnag, Y. Larger Value and SI Measurement of the Improved Cryogenic Capacitor for the Electron-Counting Capacitance Standard. *IEEE Trans. Instrum. Meas.* **2003**, *52*, 608–611.

(46) Hirano, T.; Furuhata, T.; Gabriel, K. J.; Fujita, H. Design, Fabrication, and Operation of Submicron Gap Comb-Drive Microactuators. *J. Microelectromech. S.* **1992**, *1*, 52–59.

(47) Jaecklin, V. P.; Linder, C.; de Rooij, N. F.; Moret, J. M. Micromechanical comb actuators with low driving voltage. *J. Micromech. Microeng.* **1992**, *2*, 250–255.

(48) Legtenberg, R.; Groenveld, A. W.; Elwenspoek, M. Comb-drive actuators for large displacements. *J. Micromech. Microeng.* **1996**, *6*, 320–329.

(49) Chen, C.; Lee, C. Design and modeling for comb drive actuator with enlarged static displacement. *Sens. Actuators, A* **2004**, *115*, 530–539.

(50) Gu, L.; Hunag, Q.-A.; Qin, M. A novel capacitive-type humidity sensor using CMOS fabriacation technology. *Sens. Actuators, B* **2004**, *99*, 491–498.

(51) Desai, A. V.; Haque, M. A. Design and fabrication of a direction sensitive MEMS shear stress sensor with high spatial and temporal resolution. *J. Micromech. Microeng.* **2004**, *14*, 1718–1725.

(52) Yung, K. C.; Mei, S. M.; Yue, T. M. Rapid prototyping of polymer—based MEMS devices using UV YAG laser. *J. Micromech. Microeng.* **2004**, *14*, 1682–1686.

(53) Seok, S.; Choi, W.; Chun, K. A novel linearly tunable MEMS variable capacitor. *J. Micromech. Microeng.* **2002**, *12*, 82–86.

(54) Kim, J.; Christian, D.; Lin, L. Micro Vertical comb actuators by selective stiction process. *Sens. Actuators, A* **2006**, *127*, 248–254.

(55) Hamelin, J.; Mehl, J. B.; Moldover, M. R. Resonators for accurate dielectric measurements in conducting liquids. *Rev. Sci. Instrum.* **1998**, *69*, 255–260.

(56) Hamelin, J.; Mehl, J. B.; Moldover, M. R. The static dielectric constant of liquid water between 274 and 418 K near the saturated vapour pressure. *Int. J. Thermophys.* **1998**, *19*, 1359–1380.

(57) May, E. F.; Edwards, T. J.; Mann, A. G.; Edwards, C. Dew point, liquid volume, and dielectric constant measurements in a vapour mixture of methane + propane using a microwave apparatus. *Int. J. Thermophys.* **2003**, *24*, 1509–1525.

(58) Marcuwitz, N. *Waveguide Handbook, Sec. 5.27*; McGraw-Hill: New York, 1951.

(59) Chao, S. H. Measurements of Microwave Conductivity and Dielectric Constant by the Cavity Perturbation Method and Their Errors. *IEEE T Microw. Theory* **1985**, *MTT-33*, 519–526.

(60) Dunlap, W. C.; Watters, R. L. Direct Measurement of the Dielectric Constants of Silicon and Germanium. *Phys. Rev.* **1953**, *92*, 1396–1397.

(61) Chen, X. Y.; Ma, Z.; Jensen, G. U. Lumped model for the comb-finger capacitance and electrostatic force. *Proc. SPIE* **2004**, *5641*, 130–137.

(62) Plonsey, R.; Collin, R. E. *Principles and Applications of Electromagnetic Fields.* New York: McGraw-Hill, 1961..

(63) Bansal, A.; Paul, B. C.; Roy, K. Modeling and Optimization of Fringe Capacitance of Nanoscale DGMOS Devices. *IEEE T. Electron Dev.* **2005**, *52*, 256–262.

(64) Iskander, M. F.; Stuchly, S. S. Fringing field effect in the lumped-capacitance method for permittivity measurements. *IEEE Trans. Instrum. Meas.* **1978**, *IM27*, 107.

(65) Stuchly, S. S.; Gajda, G.; Anderson, L.; Kraszewski, A. A new sensor for dielectric measurements. *IEEE Trans. Instrum. Meas.* **1986**, *IM-35*, 138–141.

(66) *ASM Metals Reference Book*; Bauccio, M., Ed.; ASM International: OH, 1993.

(67) Moldover, M. R.; Buckley, T. J. Reference Values of the Dielectric Constant of Natural Gas Components Determined with a Cross Capacitor. *Int. J. Thermophys.* **2001**, *22*, 859–885.

(68) Bourouina, T.; Spirkovitch, S.; Marty, F.; Baillieu, F.; Donzier, E. Silicon etching techniques and application to mechanical devices. *Appl. Surf. Sci.* **1993**, *65–66*, 536–542.

(69) Manrique de Lara, M. Ph.D. Thesis, Development of an Integrated Model of Vibrating Element Fluid Property Sensor, University of London, 2005.

(70) Kovacs, G. T. A.; Maluf, N. I.; Petersen, K. E. Bulk Micromachining of Silicon. *Proc. IEEE* **1998**, *86*, 1536–1551.

(71) Scaife, W. G.; Lyons, C. G. R. An equation of state based on measurements of relative dielectric permittivity. *J. Phys. D: Appl. Phys.* **1983**, *16*, 39–52.

(72) Scaife, W. G.; Lyons, C. G. R. Dielectric permittivity and pvT data of some n-alkanes. *Proc. R. Soc. London A* **1980**, *370*, 193–211.

(73) Scaife, W. G.; Lyons, C. G. R. Design of a Permittivity Cell for Liquids Subjected to High Pressures. *Rev. Sci. Instrum.* **1970**, *41*, 625–627.

(74) Scaife, W. G.; Lyons, C. G. R. Dielectric permittivity and pvT data of some n-alkanes. *Proc. R. Soc. London A* **1980**, *370*, 193–211, SUP 10031 available from the British Library.

(75) Brazier, D. W.; Freeman, G. R. Effects of Pressure on the Density, Dielectric Constant, and Viscosity of Several Hydrocarbons and Other Organic Liquids. *Can. J. Chem.* **1969**, *47*, 893–899.

(76) Böttcher, C. J. F. *Theory of Electric Polarization*, 2nd Ed.; Elsevier: Amsterdam, 1973; Vol. 1.

(77) Kirkwood, J. G. The Dielectric Polarization of Polar Liquids. *J. Chem. Phys.* **1939**, *7*, 911–919.

(78) Eltringham, W.; Catchpole, O. J. Relative Permittivity Measurements of Trifluoromethyl Methyl Ether and Pentafluoroethyl Methyl Ether. *J. Chem. Eng. Data* **2007**, *52*, 1095–1099.

(79) Barao, T.; Nieto de Castro, C. A.; Mardolcar, U. V.; Okambawa, R.; St-Arnaud, J. M. Dielectric constant, dielectric virial coefficients and dipole moments of 1,1,1,2-tetrafluoroethane. *J. Chem. Eng. Data* **1995**, *40*, 1242–1248.

(80) Owen, B. B.; Brinkley, S. T. The Effect of Pressure upon the Dielectric Constants of Liquids. *Phys. Rev.* **1943**, *64*, 32–36.

(81) Hayward, A. T. J. Compressibility equations for liquids: a comparative study. *Br. J. Appl. Phys.* **1967**, *18*, 965–977.

(82) Tammann, G. *Uber die Beziehungen zwischen den inner Kräften und Eigenschaften der Lösungen.* Voss: Liepzig, 1907; p 36.

(83) Kirkwood, J. G. The Dielectric Polarization of Polar Fluids. *J. Chem. Phys.* **1939**, *7*, 911–919.

(84) Ledbetter, H. M.; Weston, W. F.; Naimon, E. R. Low-temperature elastic properties of four austenitic stainless steels. *J. Appl. Phys.* **1975**, *46*, 3855–3859.